Rapid eccentricity oscillations and the mergers of compact objects in hierarchical triples

Joe M. Antognini,[1][*] Benjamin J. Shappee,[1] Todd A. Thompson[1,2] and Pau Amaro-Seoane[3]

[1]*Department of Astronomy, The Ohio State University, Columbus, OH 43210, USA*
[2]*Center of Cosmology and Astro-Particle Physics, The Ohio State University, Columbus, OH 43210, USA*
[3]*Max Planck Institut für Gravitationsphysik (Albert-Einstein Institut), D-14476 Potsdam, Germany*

ABSTRACT

Kozai–Lidov (KL) oscillations can accelerate compact object mergers via gravitational wave radiation by driving the inner binaries of hierarchical triples to high eccentricities. We perform direct three-body integrations of high-mass-ratio compact object triple systems using FEWBODY including post-Newtonian terms. We find that the inner binary undergoes rapid eccentricity oscillations (REOs) on the time-scale of the outer orbital period which drive it to higher eccentricities than secular theory would otherwise predict, resulting in substantially reduced merger times. For a uniform distribution of tertiary eccentricity (e_2), ∼40 per cent of systems merge within ∼1–2 eccentric KL time-scales whereas secular theory predicts that only ∼20 per cent of such systems merge that rapidly. This discrepancy becomes especially pronounced at *low* e_2, with secular theory overpredicting the merger time by many orders of magnitude. We show that a non-negligible fraction of systems have eccentricity >0.8 when they merge, in contrast to predictions from secular theory. Our results are applicable to high-mass-ratio triple systems containing black holes or neutron stars. In objects in which tidal effects are important, such as white dwarfs, stars, and planets, REOs can reduce the tidal circularization time-scale by an order of magnitude and bring the components of the inner binary into closer orbits than would be possible in the secular approximation.

Key words: binaries: close – stars: kinematics.

1 INTRODUCTION

Hierarchical triple systems are common (Raghavan et al. 2010) and exhibit dynamics that are qualitatively different from binary systems (Poincaré 1892). For example, if the tertiary is highly inclined with respect to the inner binary, it induces slow oscillations of the orbital parameters of the inner binary. In particular, the eccentricity of the inner binary oscillates between a minimum and maximum value ($e_{max} = \sqrt{1 - 5/3 \cos^2 i}$ in the limit of a test particle secondary when the three-body Hamiltonian is expanded to quadrupole order) over the time-scale (e.g. Holman, Touma & Tremaine 1997; Blaes, Lee & Socrates 2002)

$$t_{KL} \sim 1.3 \times 10^5 \, \text{yr} \left(\frac{m_1 + m_2}{2 \times 10^6 \, \text{M}_\odot} \right)^{-1/2} \left(\frac{a_1}{10^{-2} \, \text{pc}} \right)^{3/2}$$
$$\times \left(\frac{m_1 + m_2}{2m_2} \right) \left(\frac{a_2/a_1}{10} \right)^3 \left(1 - e_2^2 \right)^{3/2}. \quad (1)$$

These oscillations are known as Kozai–Lidov (KL) oscillations (Kozai 1962; Lidov 1962).

KL oscillations have found application in a wide variety of astrophysical systems including the orbits of asteroids in the Solar system (Kozai 1962), the orbits of artificial satellites around planets in the Solar system (Lidov 1962), as a formation channel for hot Jupiters (e.g. Wu & Murray 2003; Fabrycky & Tremaine 2007; Wu, Murray & Ramsahai 2007), and as a formation channel for blue stragglers (Perets & Fabrycky 2009).

KL cycles can drive the inner binary in some hierarchical triple systems to merger via gravitational wave emission (Blaes et al. 2002; Miller & Hamilton 2002). If the inner binary consists of two white dwarfs (WD), Thompson (2011) showed that these mergers occur rapidly enough to potentially explain the Type Ia supernova rate. Katz & Dong (2012) demonstrated that in a non-negligible fraction of systems, perturbations to the secular KL oscillations can drive the inner binary to collide head-on, rather than coalescing due to gravitational radiation after tidal capture (see also Prodan, Murray & Thompson 2013). Hamers et al. (2013) provide a more detailed discussion of the rates of such collisions by accounting for the evolution of the inner binary on the main sequence.

[*] E-mail: antognini@astronomy.ohio-state.edu

In addition to WD–WD mergers, KL oscillations have also been studied as a mechanism to drive other compact objects to rapid merger. Neutron star–neutron star (NS–NS) and neutron star–black hole (NS–BH) mergers have been proposed as engines of short gamma-ray bursts (Paczynski 1986; Ruffert, Janka & Schäfer 1995; Ruffert, Janka & Schaefer 1996; Janka et al. 1999; Ruffert & Janka 1999), and such mergers may also be expedited by KL oscillations (Thompson 2011). Several authors have studied mergers of stellar-mass BH, particularly in globular clusters, to determine if they can efficiently grow to intermediate-mass black holes (e.g. Miller & Hamilton 2002; Wen 2003; Gültekin, Miller & Hamilton 2004; Aarseth 2012). Hierarchical triples of supermassive black holes (SMBHs) may also merge quickly as a result of KL oscillations (Blaes et al. 2002; Hoffman & Loeb 2007; Amaro-Seoane et al. 2010). These effects can also produce interesting gravitational wave signatures from stellar-mass binaries in orbit around one or more SMBHs (e.g. Antonini & Perets 2012; Bode & Wegg 2014).

Given its general nature, the physics behind the KL mechanism has come under broader study in the past several years. Until recently, almost all work exploring it has employed the secular approximation, which assumes that any changes to the orbital parameters of the system are slow compared to the orbital period of the outer binary. The Hamiltonian is expanded in powers of the ratio of the semimajor axis of the inner binary to the semimajor axis of the outer binary (a_1/a_2), typically to quadrupole order, $(a_1/a_2)^2$. Krymolowski & Mazeh (1999) and Ford, Kozinsky & Rasio (2000, 2004) derived the equations of motion to octupole order, $(a_1/a_2)^3$ (see Naoz et al. 2013). Lithwick & Naoz (2011) and Katz, Dong & Malhotra (2011) explored the implications of these equations and showed that the octupole-order terms can lead to substantially larger eccentricities of the inner binary. This so-called eccentric Kozai mechanism (EKM) has dramatically expanded the parameter space in which mergers and other interesting dynamics can occur (e.g. Naoz, Farr & Rasio 2012; Shappee & Thompson 2013).

It is becoming increasingly evident, however, that the secular approximation can fail in certain circumstances. Antonini & Perets (2012) found that in extreme-mass-ratio systems, eccentricities change rapidly compared to the period of the tertiary if the tertiary is in an eccentric orbit (this behaviour can also be seen in Antonini et al. 2010). Bode & Wegg (2014) found that in a more general set of systems, the eccentricity of the inner binary varies on the time-scale of the orbit of the tertiary. Recently, Katz & Dong (2012) found that these rapid variations can lead to collisions of WD–WD binaries if the tertiary is at very high inclination.[1] Finally, Seto (2013) examined the impact of these rapid fluctuations on gravitational wave astronomy.

In this paper, we revisit earlier calculations of the merger times of compact objects by Blaes et al. (2002) and Hoffman & Loeb (2007). We extend these works by directly integrating the equations of motion of the three-body system and including post-Newtonian (PN) force terms up to order 3.5 to account for general relativistic (GR) effects. We show that motion of the tertiary on its orbit (even in relatively low eccentricity orbits) leads to rapid eccentricity oscillations (REOs) in the inner binary and we quantify the

importance of these oscillations. Our goal is to better understand the effect of the eccentric KL mechanism and non-secular effects on the merger time distribution and dynamics of compact object binaries. In systems with tertiaries in low-eccentricity orbits, we find that the double-orbit-averaged secular approximation fails by predicting merger times many orders of magnitude longer than those of the direct three-body integration.

This paper is structured as follows. In Section 2, we describe our numerical methods and characterize the accuracy of our integration (see also the appendix). In Section 3, we describe the breakdown of the secular approximation in calculating the eccentricity of the inner binary. In Section 4, we demonstrate one regime in which this breakdown of the secular approximation leads to catastrophic failure, namely in predicting the merger times of compact objects. We conclude and discuss a number of applications in Section 5.

As this paper was being completed, Antonini, Murray & Mikkola (2014) presented similar results on the breakdown of the secular approximation, the delay time distribution, and the eccentricity distribution of compact object binaries at merger.

2 NUMERICAL METHODS AND SETUP

We numerically evolve triple systems with the open source FEWBODY suite (Fregeau et al. 2004). FEWBODY is designed to compute the dynamics of hierarchical systems of small numbers of objects ($N \lesssim 10$) either in scattering experiments or in bound systems. The underlying integrator for the FEWBODY suite is the GNU Scientific Library (GSL) ordinary differential equations library (Gough 2009). By default FEWBODY uses eighth-order Runge–Kutta Prince–Dormand integration with adaptive time steps. It is straightforward to modify FEWBODY to use any of the other roughly half-dozen integration algorithms supported by GSL.[2] In our experience, the choice of integration algorithm does not affect the results since the adaptive steps force the size of the error to be within the same target value regardless of the algorithm used. All results in this paper were obtained using the default eighth-order Runge–Kutta Prince–Dormand algorithm. To incorporate relativistic effects, we have included PN terms up to order 3.5 in the integration. Details of energy conservation, gravitational radiation, and a comparison to secular calculations are provided in Appendix A. These additions to FEWBODY and a direct application to the formation of gravitational-wave sources for ground-based detectors will be presented in more detail in Amaro-Seoane (in preparation).

Throughout this paper, we use m_1 and m_2 to refer to the masses of the objects in the inner binary, and m_3 to refer to the mass of the tertiary. For other quantities the subscript '1' refers to the inner binary and the subscript '2' refers to the outer binary. The semimajor axis is represented by a, the eccentricity by e, the argument of periapsis by g, and the mutual inclination by i.

3 RAPID ECCENTRICITY OSCILLATIONS

Most studies of three-body dynamics have employed the secular approximation in which any changes to the orbital parameters of either orbit are assumed to be slow compared to the orbital period of both orbits. Such models cannot account for any changes that

---

[1] Katz & Dong (2012) distinguish between 'head-on collisions', in which two objects merge without substantial tidal interaction, and 'collisions', in which two objects merge with or without previous tidal interaction. We use 'collision' to refer exclusively to mergers without tidal interaction. Any event in which the two objects undergo substantial tidal interaction before combining is termed a 'merger' in this paper.

[2] GSL also supports an additional five integration algorithms, but these require the calculation of the Jacobian. When PN terms are included this becomes non-trivial to implement.
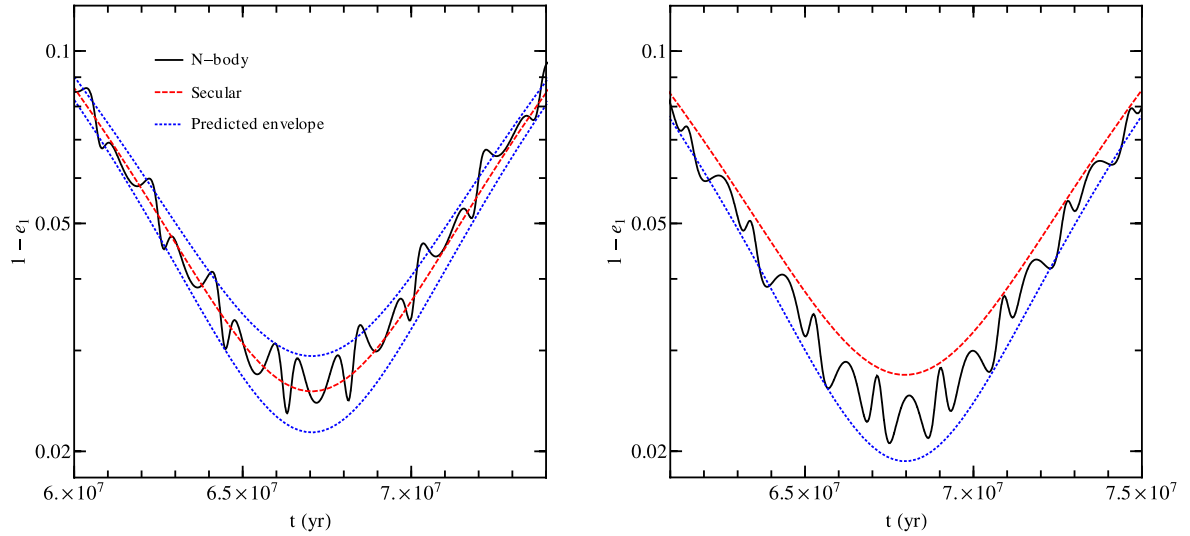
Figure 1. Systems exhibiting REOs. The eccentricity of the inner binary during a KL cycle as calculated by direct three-body integration (black solid line) and as calculated in the secular approximation (red dashed line) for $g_1 = g_2 = 0°$ (left-hand panel) and $g_1 - g_2 = 90°$ (right-hand panel). PN terms are not included. The secular and three-body calculations match on average in the left-hand panel, but the three-body calculation exhibits oscillations in e_1. In the right-hand panel, the secular calculation correctly predicts the minimum eccentricity, but the REOs in the three-body calculation push the binary exclusively to higher eccentricities. Blue dotted lines show the amplitude of the REOs predicted by equation (2). The period of the REOs is twice the period of the outer binary. The asymmetry in the period of the oscillations is due to fact that the tertiary is on an eccentric orbit ($e_2 = 0.2$). The initial conditions of the system are presented in Table 1 but with g_1 and g_2 fixed as stated above.

Table 1. Initial conditions for triple systems studied in this paper. Throughout this paper, g refers to the argument of periapsis and i refers to the mutual inclination.

m_1	m_2	m_3	a_1	a_2	e_1	e_2	g_1	g_2	i
$10^7\,\mathrm{M_\odot}$	$10^5\,\mathrm{M_\odot}$	$10^7\,\mathrm{M_\odot}$	1 pc	20 pc	0.1	0.1–0.8	0°–360°	0°–360°	80°

occur on more rapid time-scales, and it is implicitly assumed that if such changes do occur, their effect would be negligible.

We find that over a broad region of parameter space, the inner binaries in triple systems undergo oscillations in eccentricity (or, equivalently, angular momentum) on the time-scale of the outer orbital period ('rapid eccentricity oscillations', REOs). REOs are typically small and do not affect the dynamics of the triple system for almost all of its evolution. But when the inner binary is already at high eccentricity, as during an eccentric Kozai cycle, the magnitude of the oscillations in angular momentum becomes comparable to the total angular momentum of the inner binary. REOs can then drive the inner binary to rapid merger.

The existence of REOs was predicted by Ivanov, Polnarev & Saha (2005), who found that the amplitude of the change in angular momentum during an oscillation is

$$\frac{\Delta L}{\mu} = \frac{15}{4} \frac{m_3}{m_1 + m_2} \cos i_{\min} \left(\frac{a_1}{a_2}\right)^2 \sqrt{Gm_3 a_2}, \quad (2)$$

where μ is the reduced mass of the inner binary and $i_{\min}$ is the minimum mutual inclination between the two orbits during a KL cycle.[3] Equation (2) can also be written as a change in eccentricity,

---

[3] See appendix B of Ivanov et al. 2005 for the complete derivation. Note that in Ivanov et al. 2005, ΔL refers to the change in the specific angular momentum from the average value to the maximum value. This quantity therefore differs from our ΔL by a factor of $\mu/2$.

although this form of the equation is somewhat more cumbersome:

$$\Delta e_1 = -e_1$$
$$+ \sqrt{1 - \left[\sqrt{1 - e_1^2} + \frac{15}{4}\left(\frac{m_3}{m_1 + m_2}\right)^{3/2} \cos i_{\min} \left(\frac{a_1}{a_2}\right)^{3/2}\right]^2}. \quad (3)$$

These equations are only accurate near the eccentricity maximum of a KL cycle.

Our numerical experiments are in agreement with Ivanov et al. (2005). We show in Fig. 1 the evolution of two example systems exhibiting REOs (see Table 1). The two systems are identical except that the system in the left-hand panel begins with $g_1 = g_2 = 0°$ and the right-hand panel begins with $g_1 - g_2 = 90°$. To demonstrate that REOs are a non-relativistic phenomenon, we have suppressed PN terms in this figure.

Intuitively, REOs can be understood as similar to a KL oscillation in miniature. In the double-orbit-averaged approximation, the KL mechanism occurs due to the fact that the outer orbit exerts a stronger force on the inner orbit at the line of nodes than at other regions of the outer orbit. But because in reality the outer orbit is a point mass in motion rather than a continuous hoop of matter, this force is strongest along the line of nodes as the tertiary is actually passing through the line of nodes. For weak KL oscillations, the driving force contributed during any single orbit is small, so there is only a gradual change in the eccentricity of the inner orbit and any REOs are negligible. However, during a strong eccentricity maximum,

the inner orbit has lost nearly all of its angular momentum and is therefore extremely sensitive to torquing.

This implies that the arguments of periapsis of the inner and outer orbits determine the direction of the oscillation. If the apsides are aligned with the line of nodes (as in the left-hand panel of Fig. 1), the eccentricity will be driven to higher values relative to the secular calculation when the tertiary passes through periapsis and to lower values when the tertiary passes through apoapsis. If the apsides are 90° from the line of nodes, however, the eccentricity will be exclusively driven to higher values relative to the secular calculation while the amplitude of the oscillations will remain fixed (as in the right-hand panel of Fig. 1).

Although oscillations in the orbital elements on the time-scale of the period of the outer orbit were first predicted by Soderhjelm (1975), an explicit formula for the change in angular momentum was first derived by Ivanov et al. (2005). Moreover, these oscillations were not confirmed by three-body integrations until Bode & Wegg (2014), who found them in the test-particle limit, and Antonini & Perets (2012), who found them in the equal-mass case. Katz & Dong (2012) further explored these oscillations in the context of WD–WD collisions. They argued that these oscillations are fundamentally a stochastic phenomenon, but only examined systems in which the inclination of the tertiary was near the Kozai 'pole' of $i \sim 93°$, where certain terms in the Hamiltonian formally diverge at quadrupole order and KL oscillations become extremely strong (Miller & Hamilton 2002). Although a complete analytic treatment of REOs is beyond the scope of this paper, our results suggest that at lower inclinations they could be modelled analytically. As we discuss in Section 4.2, we only examine REOs in inner binaries on prograde orbits.

4 EFFECT ON MERGER TIMES

REOs are important when $1 - e_1 \sim 0$ and nearly all of the angular momentum in the inner orbit has been transferred to the outer orbit. Here, fluctuations in the angular momentum given by equation (2) become comparable to the total angular momentum in the inner orbit itself. REOs then can have a substantial impact on the long-term dynamics. This is especially true if relativistic effects are important because the PN terms are strong functions of distance and thus a small change in the distance at periapsis dramatically changes their strength. A secular calculation does not account for these effects and will overpredict the merger time, in some cases by many orders of magnitude. There are therefore certain regions of parameter space in which the double-orbit-averaging approximation fails.

4.1 Test case

The importance of REOs for the long-term evolution of an example system is illustrated in Fig. 2. The secular calculation (red dashed line) closely matches the three-body integration performed by FEWBODY (black line) during the first KL cycle, but afterwards they begin to diverge. In this particular case, the eccentricity of the inner binary in the three-body integration increases to $1 - e_1 < 10^{-4}$, whereas in the secular calculation it only reaches $1 - e_1 \sim 10^{-3}$. As a consequence, the three-body integration predicts the inner binary to merge within one eccentric-KL time-scale whereas the secular calculation predicts that the inner binary will effectively never merge. To demonstrate the importance of resonant PN eccentricity excitation (Naoz et al. 2013b), we additionally show the same three-body calculation without any PN terms (blue dotted line). We find that
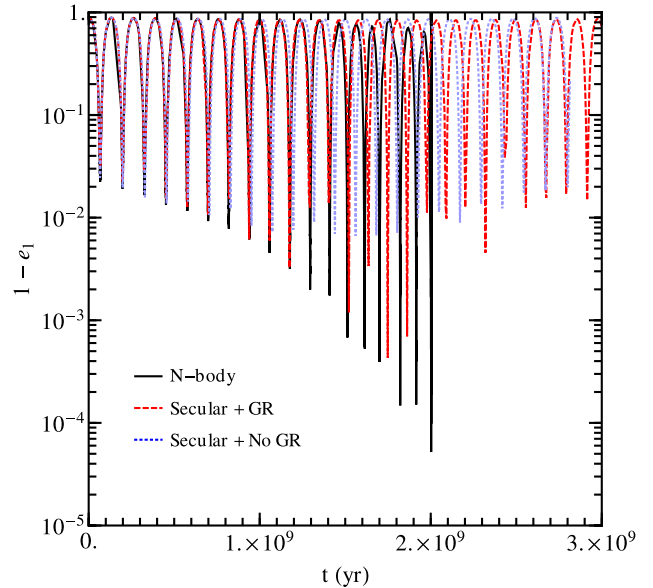

Figure 2. The impact of REOs on the evolution of the inner binary of a hierarchical triple. We show the direct three-body integration (solid black line) and the calculation in the secular approximation (red dashed line). To illustrate the importance of relativistic terms at high eccentricities, we also show the direct three-body integration without any PN terms (blue dotted line). Although the direct integration matches closely with the two secular calculations during the first KL cycle, the calculations diverge thereafter. The secular calculation predicts that the system only reaches a maximum eccentricity of $1 - e_1 \sim 10^{-3}$ in the time period shown, whereas the direct integration predicts that the inner binary is driven to sufficiently high eccentricities to merge after $\sim 2 \times 10^9$ yr.

without relativistic effects the inner binary gets excited to much lower eccentricities, in agreement with Naoz et al. (2013b).

During the eccentric phase of the KL cycles the GR precession time-scale, t_{GR}, shortens since e_1 approaches unity (e.g. Blaes et al. 2002):

$$t_{GR} \sim 2.3 \times 10^6 \text{ yr} \left(\frac{m_1 + m_2}{2 \times 10^6 \, M_\odot} \right)^{-3/2} \left(\frac{a_1}{10^{-2} \, pc} \right)^{5/2} \left(1 - e_1^2 \right).$$
(4)

If the eccentricity becomes sufficiently large, as in the final KL cycles of the system presented in Fig. 2, t_{GR} can become shorter than the KL time-scale, t_{KL} (equation 1). This will ordinarily not suppress the KL mechanism because at high eccentricity the inner binary requires only very small torques to change its eccentricity. Bode & Wegg (2014) therefore introduce the *instantaneous* KL time-scale, $t_{KL, \, inst}$ as the time-scale for the inner binary to change its angular momentum by order unity. $t_{KL, \, inst}$ is related to t_{KL} by

$$t_{KL,inst} \sim \sqrt{1 - e_1^2} \, t_{KL}$$
(5)

up to constant factors of order unity. If $t_{KL, \, inst}$ exceeds t_{GR} the KL cycles are 'detuned', and the KL mechanism will be suppressed (Holman et al. 1997). This kind of detuning occurs in the regime in which the secular approximation is valid. The detuning which occurs in the system presented in Fig. 2 does not occur in this regime, however. In this system, t_{GR} becomes shorter than P_2 before it becomes shorter than $t_{KL, \, inst}$. When this occurs, it is impossible
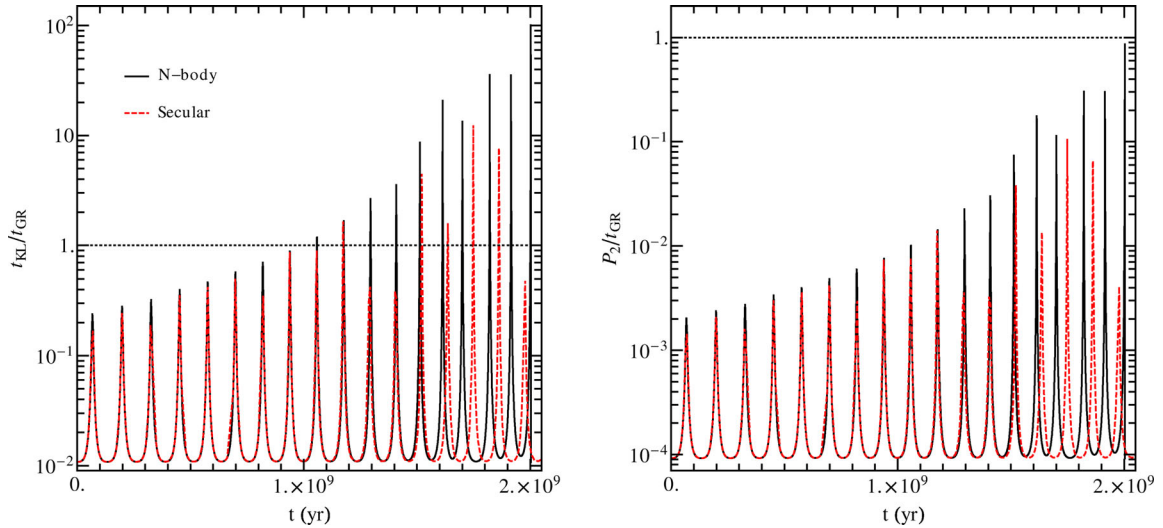
Figure 3. Timescales of the system presented in Fig. 2 calculated with direct integration (black line) and in the secular approximation (dotted red line). *Left-hand panel.* The ratio between the KL time-scale (equation 1) and the GR precession time-scale (equation 4) of the inner binary. During the final several KL cycles the GR precession time-scale becomes shorter than the KL time-scale. Although the KL mechanism is detuned, REOs are sufficient to restore the system to lower eccentricities and continue the KL cycle. *Right-hand panel.* The ratio between the outer period and the GR precession time-scale. Once the GR precession time-scale of the inner binary becomes comparable to the outer orbital period, the two orbits completely decouple and gravitational radiation drives the inner binary to merge.

for the outer binary to exert any secular influence on the inner binary. At this point, the inner binary decouples from the outer binary and gravitational radiation drives the inner binary to rapid merger because the inner binary is at high eccentricity. Hence, the KL mechanism is detuned as a consequence of the breakdown of the secular approximation. To emphasize that t_{KL} is not relevant for determining if KL cycles will be detuned in the middle of a KL cycle, we show in the left-hand panel of Fig. 3 the ratio between t_{KL} and t_{GR} for the system presented in Fig. 2. During the final KL cycles t_{GR} becomes much shorter than t_{KL}, but is driven back to longer time-scales by REOs before the inner binary can merge by gravitational radiation. The right-hand panel shows the ratio between P_2 and t_{GR} for the same system. Once this ratio reaches unity, the inner binary decouples from the outer binary and merges via gravitational radiation.

We emphasize that REOs are only important when the eccentricity is large. REOs therefore only affect the dynamics during a small fraction of the system's lifetime. We illustrate in Fig. 4 the fraction of time that the system spends at high eccentricity. The fluctuations in the angular momentum of the inner binary become 10 per cent of the total angular momentum of the inner binary when the inner binary reaches an eccentricity of ∼0.9. From Fig. 4, REOs are therefore non-negligible for only ∼10 per cent of the system's lifetime. The secular approximation is therefore valid ∼90 per cent of the time. Nevertheless, as illustrated in Fig. 2 and in the next subsection, these short periods in which the secular approximation fails dramatically influence the evolution of the system and lead to a sharp divergence from the secular predictions because of the strong eccentricity dependence of the GR terms.

4.2 Population study

Here, we compare the merger times of a variety systems calculated in both the secular approximation and in the full three-body integration. We fix the masses of the SMBHs ($m_1 = 10^7 \, M_\odot$, $m_2 = 10^5 \, M_\odot$, $m_3 = 10^7 \, M_\odot$), the semimajor axes ($a_1 = 1 \, \text{pc}$, $a_2 = 20 \, \text{pc}$), the initial eccentricity of the inner binary ($e_1 = 0.1$),
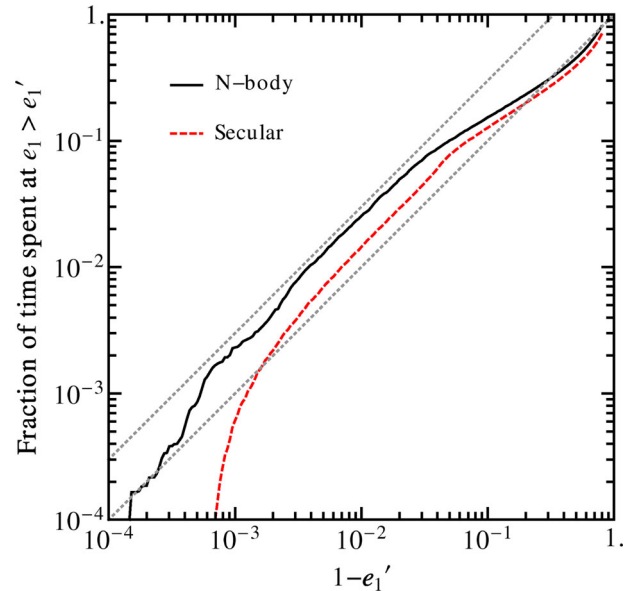

Figure 4. The fraction of time that the system presented in Fig. 2 spends at eccentricities greater than any given eccentricity in the direct integration (solid line) and in the secular approximation (red dashed line). For comparison, we also present the line $y = x$ and $y = 3x$ (dotted lines). At low eccentricities, the fraction of time that a hierarchical triple undergoing KL cycles spends at eccentricities greater than e_1 is approximately $1 - e_1$. REOs drive the system to spend more time at higher eccentricities. If eccentric KL oscillations are also present, as in this case, the fraction of time spent at higher eccentricities is slightly larger, but is always within a factor of a few of $1 - e_1$. Although REOs are only important at high eccentricities, their effect during these brief periods drastically changes the overall evolution of the system.

the inclination of the tertiary ($i = 80°$), and the arguments of periapsis ($g_1 = 0°$, $g_2 = 90°$). The initial mean anomalies are chosen randomly. The eccentricity of the tertiary, e_2, is systematically varied from $e_2 = 0.1$ to 0.85 in steps of 0.001. (Systems at $e_2 \gtrsim 0.85$
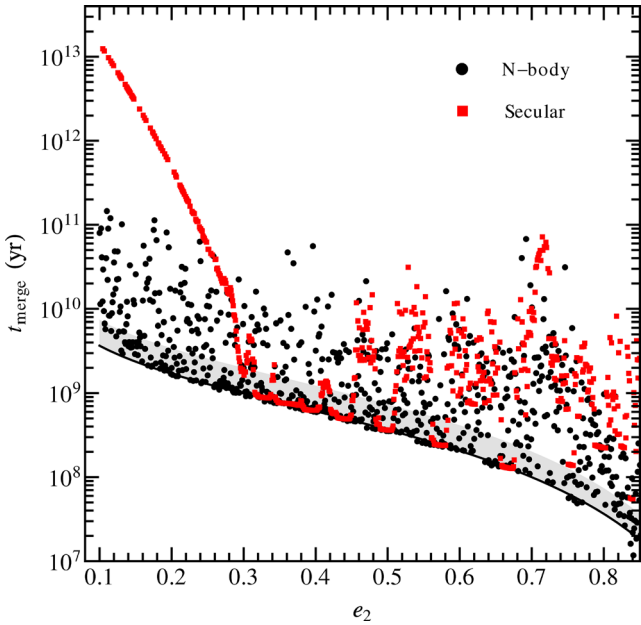
Figure 5. The time required for the inner binary of triple systems to merge as a function of the eccentricity of the orbit of the tertiary (see Table 1 for the system parameters) using direct three-body integrations (points) and using the secular approximation (red dashed line). The scatter in both the direct three-body integration and in the double-orbit-averaged calculation is due to the fact that these systems are chaotic. Slight changes in e_2 or the initial mean anomalies can change t_{merge} by over an order of magnitude. Approximately 25 per cent of the systems we study merge in t_{EKM} (equation 6, solid line). The shaded region depicts merger times within $1-2 \times t_{\mathrm{EKM}}$. At $e_2 \lesssim 0.3$ the eccentric KL mechanism weakens and cannot drive systems to merger as shown by the large difference between the secular and three-body calculations. As a consequence, REOs become an important mechanism to drive binaries to merger. Because REOs are fundamentally non-secular, the secular calculations overpredict the merger times by many orders of magnitude at low e_2.

are unstable and few systems with $e_2 \lesssim 0.1$ ever merge.) Note that we do not choose our masses to model any specific physical system (the REO phenomenon is not specific to any particular mass range), but instead choose them for ease of comparison to Blaes et al. (2002), and because we wish to study this phenomenon in the test-particle case.

At each choice of e_2 we calculate the merger time. We define a merger as occurring when the two components of the inner binary come within 10 Schwarzschild radii (R_{Sch}) of each other (where R_{Sch} hereafter refers to the Schwarzschild radius of the larger BH). We are forced to integrate only to $10\,R_{\mathrm{Sch}}$ rather than down to 1 or $2\,R_{\mathrm{Sch}}$ because the PN terms begin diverging when the relative velocity exceeds $\sim 0.2c$ (see section 9.6 of Blanchet 2006). In the systems we examine, the relative velocities start to become close to $\sim 0.2c$ when the two components come within $10\,R_{\mathrm{Sch}}$ of each other. In practice, when the inner objects come within $10\,R_{\mathrm{Sch}}$ of each other, the orbital decay time-scale is short compared to the overall merger time.[4]

The results of these calculations appear in Fig. 5. Because these orbits spend the vast majority of time in the Newtonian regime,

they can be rescaled to other masses, distances, and times until the small fraction of time prior to merger that the eccentricity becomes large enough that relativistic effects become important. For this reason, we run each calculation to completion even if the merger time exceeds a Hubble time for the particular case that we analyse.

There is substantial scatter in t_{merge}. This scatter is a result of the slightly different choices of e_2 from point to point, but also the different mean anomalies. Two systems with identical starting conditions but different initial mean anomalies can have merger times that differ by up to two orders of magnitude. The most rapidly merging systems all merge within one eccentric KL time-scale. This time-scale is given by Katz et al. (2011) and Naoz et al. (2013) as

$$t_{\mathrm{EKM}} \sim \frac{t_{\mathrm{KL}}}{\epsilon_{\mathrm{oct}}},$$

where ϵ_{oct} is the strength of the octupole-order term in the expansion of the three-body Hamiltonian. The eccentric KL time-scale can be written as

$$t_{\mathrm{EKM}} \sim 2.1 \times 10^9\,\mathrm{yr} \left(\frac{m_1 + m_2}{2 \times 10^6\,\mathrm{M}_\odot} \right)^{-1/2} \left(\frac{a_1}{1\,\mathrm{pc}} \right)^{3/2}$$

$$\times \left(\frac{m_1 + m_2}{2m_3} \right) \left(\frac{a_2/a_1}{20} \right)^4 \frac{(1 - e_2^2)^{5/2}}{e_2}. \tag{6}$$

This function matches the lower envelope of the merger time distribution very closely. Systems above this line fail to merge within a single eccentric KL cycle, but merge after several. Usually, however, the first eccentric KL cycle so disturbs the system that future eccentric KL cycles operate on different time-scales. This is primarily due to changes in the argument of periapsis of the inner binary. The merger times are therefore not integer multiples of the first eccentric KL time-scale.

Of the systems we study, approximately one-quarter merge within one eccentric KL cycle. This is an overestimate of the true fraction of systems that merge within t_{EKM} since we study only a small region of parameter space. Although our choice of inclination ($i = 80°$) is not finely tuned, our choice of arguments of periapsis ($g_1 = 0°$, $g_2 = 90°$) is tuned to encourage strong eccentric KL resonances. We do this for two reasons. First, it is computationally expensive to integrate a sufficient number of systems to marginalize over the arguments of periapsis and obtain good statistics. Secondly, it demonstrates more clearly that the lower envelope of the t_{merge} distribution is set by t_{EKM} because both KL resonances and REOs are stronger when the arguments of periapsis are different by $90°$.

To examine the effect of a more realistic distribution of initial arguments of periapsis on the merger time distribution, we pick two choices of e_2 (0.2 and 0.6), and calculate the evolution of 100 systems with uniform distributions of g_1 and g_2. We compare this distribution of t_{merge} (black line) to the distribution when the arguments of periapsis are fixed to $g_1 = 0°$ and $g_2 = 90°$ (blue dashed line) in Fig. 6. As expected, the distribution shifts to longer merger times when the arguments of periapsis are chosen randomly. Nevertheless, about ~ 15 per cent of systems with $e_2 = 0.2$ and about ~ 30 per cent of systems with $e_2 = 0.6$ merge within a few $\times t_{\mathrm{EKM}}$. We additionally compare this result to that calculated in the secular approximation and find that it is shifted to much longer t_{merge} than either calculation performed using direct three-body integration.

Double-orbit averaging fails to correctly predict the merger times most drastically for triple systems in which the tertiary is at low eccentricity. At best, the secular calculation overpredicts the merger time by two orders of magnitude, and at worst it overpredicts the merger time by nearly four. The catastrophic failure of
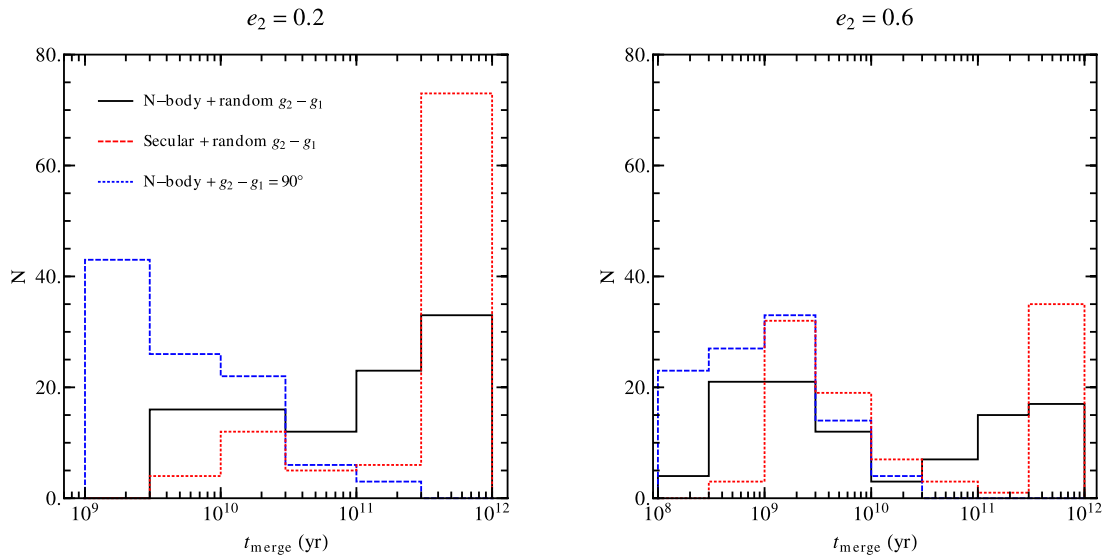
---

[4] To verify this, we reran the system displayed in Fig. 2 and set the merger criterion to 100, 50, 20, 10, and 5 Schwarzschild radii. The overall merger times are all within ~ 0.01 per cent of each other.

Figure 6. Merger time distribution for fixed e_2. We compare the distribution when the arguments of periapsis are chosen randomly from a uniform distribution (solid line) to when the arguments of periapsis are fixed at $g_1 = 0°$ and $g_2 = 90°$ calculated using direct three-body integration (blue dashed line) and in the secular approximation with a uniform distribution of arguments of periapsis (red dotted line) for 100 systems. Since KL oscillations and REOs are stronger when the arguments of periapsis differ by $90°$, the merger time distribution shifts to longer merger times when the arguments of periapsis are chosen randomly. About $15-30$ per cent of systems still merge rapidly when the arguments of periapsis are chosen randomly. The last bin of the secular calculation is a lower bound. The distribution is shifted to larger merger times when the secular approximation is employed.

double-orbit averaging is due to the fact that it cannot account for REOs. When the orbit of the tertiary has a low eccentricity, KL resonances (including eccentric KL resonances) are weakened. Consequently, when the outer orbit is at sufficiently low eccentricities, the KL resonance is not strong enough to drive the inner binary to merger on its own. KL resonances nevertheless drive the inner binary to sufficiently high eccentricities that REOs become important. REOs drive the inner binary to higher eccentricities, thereby causing relativistic effects to become much more important. In particular, gravitational wave radiation is much more efficient when the inner binary is at higher eccentricities.

5 DISCUSSION AND CONCLUSIONS

We have performed an exploration of a dynamical effect in hierarchical triple systems that is not captured by secular double-orbit averaging. By directly integrating the orbits of the three bodies and including PN terms up to order 3.5, we show that the eccentricity of the inner binary oscillates on the time-scale of the period of the outer binary with amplitude given by equations (2) and (3) (see Fig. 2 and Ivanov et al. 2005; Bode & Wegg 2014). During most of the evolution of the triple system these oscillations are negligible and secular calculations are valid. However, when the eccentricity of the inner binary is close to unity, fluctuations in the angular momentum of the inner binary due to REOs become comparable to the total angular momentum in the inner binary itself. This is because the system spends more time at higher e_1 (see Fig. 4). We find that the time spent at eccentricities greater than any given eccentricity e_1' is $\sim$few $\times (1 - e_1')$. As a consequence of this, REOs can substantially affect the dynamics of the triple system. Though we have limited our analysis in this paper to triples of SMBHs for concreteness, our results apply generally to any triple system for which the inner binary consists of BH or NS. Because relativistic effects are extremely strong functions of eccentricity, REOs can drive binaries to merge more rapidly by many orders of magnitude. As this dis-

crepancy occurs over a broad range of parameter space, REOs will drive many systems to merge which otherwise would not merge within a Hubble time. Though a complete treatment of the delay time distribution of compact object mergers across a broad range of parameter space is beyond the scope of this paper, REOs may be an important correction to calculations of the merger rate and delay time distribution of compact object binaries in triple systems (e.g. Thompson 2011; Katz & Dong 2012) and perhaps systems like stars and planets that may be strongly affected by tides (see Fig. 5 and Section 5.3 below).

5.1 Implications for extreme-mass-ratio inspirals

Since we have examined hierarchical triples with extreme mass ratios, a potential application of our results is to extreme-mass-ratio inspirals (EMRIs). EMRIs consist of a binary of stellar-mass objects in orbit around an SMBH (see, e.g. Amaro-Seoane et al. 2007; Amaro-Seoane 2012; Amaro-Seoane et al. 2013a). In such cases, there is an extremely large mass ratio between the tertiary and the inner binary. Although we ignore many important features of real EMRIs (e.g. a stellar background, which leads to several important phenomena, such as the Schwarzschild barrier, discussed in Amaro-Seoane 2012, but also the role of the spin of the central MBH; Amaro-Seoane, Sopuerta & Freitag 2013b), we here discuss the potential impacts of REOs on EMRIs as a motivation to future works. Because the amplitude of the eccentricity oscillations given by equation (2) is proportional to the mass ratio, arbitrarily large mass ratios can lead to arbitrarily large eccentricity oscillations. If the oscillations are too large they can unbind the inner binary. But encounters at large enough distances that the binary system does not become unbound could therefore lead to REOs with amplitudes comparable to the amplitude of the KL resonance itself. Eccentricity oscillations for a fiducial EMRI are shown in Fig. 7. At the peak of the KL cycle the oscillations reduce the distance at periapsis of the inner binary by over a factor of 5. Since the gravitational
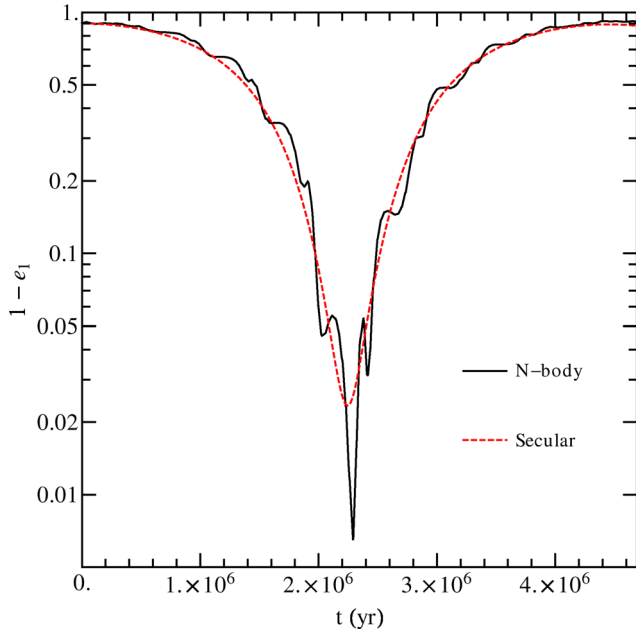
Figure 7. REOs in an EMRI calculated with direct three-body integration (solid line) and in the secular approximation (red dashed line). Because the mass ratio between the inner binary and outer binary is very large, the amplitude of the fluctuations in the angular momentum in the inner binary due to REOs becomes comparable to the angular momentum in the inner binary itself. Parameters of the system are provided in Table 1, but with $m_3 = 3 \times 10^8 \, M_\odot$, $g_1 = 0°$, $g_2 = 90°$, and $e_2 = 0.2$.

wave merger time-scale for a very eccentric orbit is proportional to $(1 - e^2)^{7/2}$ (Peters 1964), this reduction in the distance at periapsis due to REOs could lead to a significant reduction in the merger time and increase gravitational wave luminosity if the dynamical features of realistic EMRIs do not suppress this effect. These results should be studied with more detail in the context of secular effects in semi-Keplerian systems with relativistic corrections, such as in the works of Merritt et al. (2011), Brem, Amaro-Seoane & Sopuerta (2014).

5.2 Implications for gravitational wave emission

In this subsection, we discuss an important application of our findings that will be soon expanded in a statistical study of the dynamics and the implications for ground-based gravitational wave detectors such as Advanced LIGO/VIRGO, along with the detailed description of the modification of the integrator to incorporate relativistic effects (Amaro-Seoane, in preparation).

It is uncertain what the dynamics immediately prior to merger will be in systems dominated by REOs. Although the orbit will have substantially circularized by the time the two objects of the inner binary come within $10 \, R_{\rm Sch}$ of each other, the orbit nevertheless retains a non-negligible eccentricity ($e_1 \sim 0.1$) in most systems (Wen 2003; Gould 2011). Whether or not typical compact object binaries retain non-negligible eccentricity immediately prior to merger is of key importance to gravitational wave detectors like LIGO and LISA. Because these experiments require gravitational wave templates to find gravitational wave signals in their data, accurate a priori predictions of the waveform shapes are crucial for the success of these experiments. Gravitational wave searches like LIGO have generally assumed that by the time a merging binary is emitting gravitational waves at frequencies to which they are sensitive, it

has completely circularized. But if a substantial number of compact object binaries are driven to merger due to KL resonances, then the assumption of perfectly circular inspirals will be mistaken. Since gravitational radiation is a very strong function of distance, even a modest residual eccentricity ($e_1 \gtrsim 0.1$) would suffice to bury a gravitational wave signal in the data if a circular orbit template is used (Brown & Zimmerman 2010).

We calculate the eccentricity distribution of the inner binaries of the triple systems investigated in Section 4.2. Fig. 8 presents the distribution of e_1 as the two components of the inner binary come within $10 \, R_{\rm Sch}$ of each other calculated using direct three body integration (solid line) and in the secular approximation (red dashed line). At $10 \, R_{\rm Sch}$, a Keplerian orbit becomes an increasingly poor approximation to the true orbit of the inner binary. As such, we define the eccentricity of the orbit to be

$$e_1 \equiv \sqrt{1 - \frac{1}{G(m_0 + m_1)a_1}\left(\frac{L_1}{\mu_1}\right)^2}, \qquad (7)$$

where L_1 is the angular momentum of the inner binary and μ_1 is the reduced mass of the inner binary. We add PN corrections to L_1 up to second order (e.g. Iyer & Will 1995). To increase the computational efficiency, in the secular approximation we calculate systems until a_1 has decreased to 1 per cent of its initial value. At this point, the inner binary has decoupled from the outer binary and can be calculated independently. We then calculate the eccentricity of the orbit when the two components come within $10 \, R_{\rm Sch}$ of each other using the adiabatic calculation of Peters (1964).

The eccentricity distribution calculated using direct integration predicts that ~ 10 per cent of systems merge at high eccentricity ($e_1 > 0.8$). In the secular approximation, however, nearly all systems merge at low eccentricity ($e_1 \lesssim 0.2$). We also present the distribution of e_1 at $10 \, R_{\rm Sch}$ as a function of e_2 in the right-hand panel of Fig. 8. Triples with larger e_2 have a greater chance of merging at high eccentricity. Since we assume a uniform distribution of e_2 in the left-hand panel of Fig. 8, a more realistic thermal distribution will lead to a larger fraction of systems merging at high eccentricity. Population synthesis studies of hierarchical triple systems which employ the secular approximation will therefore miss an important source of unique gravitational waveforms. If an important residual eccentricity was indeed typical in these situations, gravitational wave experiments would possibly have to take this into account in the preparation of the waveform banks. This question is addressed in detail in Amaro-Seoane (in preparation).

One interesting possible outcome of an NS–NS merger in a triple system would be a head-on collision similar to those between WD described in Katz & Dong (2012). In the case of binaries consisting of objects more compact than WD, however, the chance of a collision is much smaller. This is due to two factors. First, the objects themselves have a smaller cross-section than do WD by a factor of $\sim 10^{6-7}$. Secondly, close encounters will lead to circularization of the orbit at larger distances relative to the object's radius due to the stronger relativistic effects. Head-on collisions between pairs of NS or BH should therefore be rarer than collisions between WD–WD binaries by a large factor.

5.3 Tides and implications for stars and planets

Another well-known class of triple systems with high mass ratios is that of planets in binary star systems. The formation of hot Jupiters is a long-standing problem in the theory of planet formation and KL cycles have been proposed as a mechanism to drive planets formed
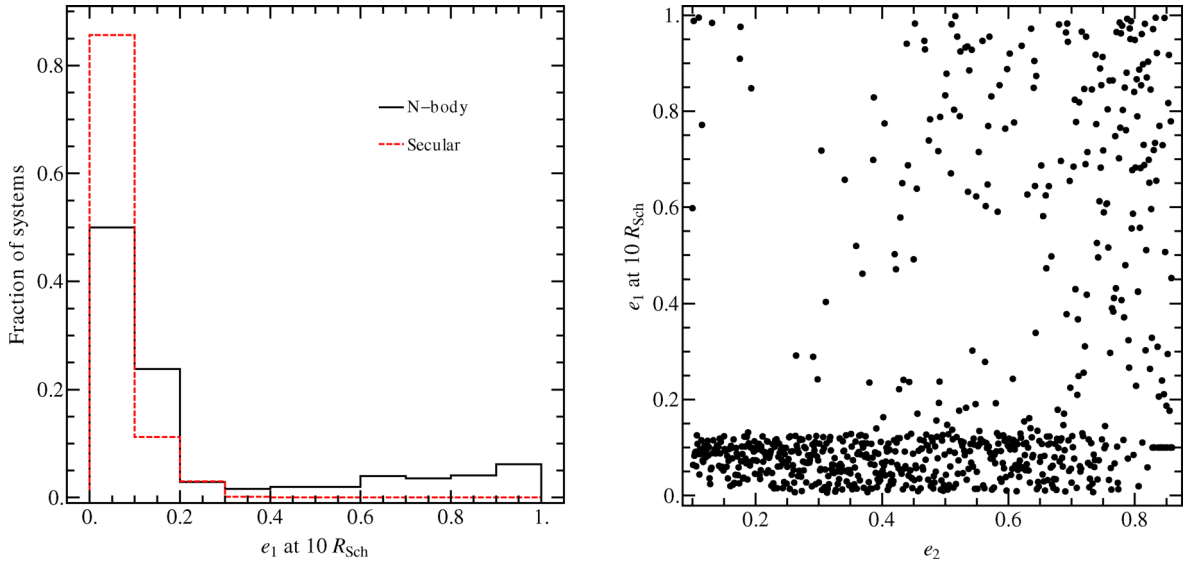
Figure 8. The eccentricity distribution of the inner orbit when the inner two components of the systems calculated in Fig. 5 come within $10\,R_{\rm Sch}$ of each other. *Left-hand panel:* the secular approximation (red dashed line) underpredicts the number of binaries which merge at high eccentricities ($e \gtrsim 0.2$) relative to the direct integration (black line). In particular, the secular approximation predicts that no binaries will come within $10\,R_{\rm Sch}$ at $e_1 > 0.4$, whereas the direct integration predicts that $\sim$20 per cent of hierarchical triples do. *Right-hand panel:* the distribution of $e_{\rm final}$ as a function of e_2. A larger fraction of systems merge at high $e_{\rm final}$ when e_2 is large. Note that we have assumed a uniform distribution in e_2; if e_2 is distributed thermally more systems will merge at high e_1. Gravitational wave detectors will need to employ templates of eccentric binaries to detect such systems.

far from the host star into tight orbits (Wu et al. 2007). Tidal effects are very important for stellar and planetary systems and while a complete treatment is beyond the scope of this paper (though see Naoz et al. 2012 for a discussion of the effect of tides on KL cycles), we nevertheless make some qualitative statements about the impact of tides on our results and the implications for stars and planets.

The overall effect of tides on eccentric orbits is to circularize them and reduce the semimajor axis (Hut 1981) on a characteristic tidal friction time-scale $t_{\rm TF}$. If the eccentricity is very close to unity, $t_{\rm TF} \propto (1 - e_1)^{-3/2}$ (Hut 1982). Tides therefore prevent stars and planets from remaining on high-eccentricity orbits for long periods of time and will disrupt sufficiently strong KL cycles. However, REOs occur on a shorter time-scale than the KL cycle by a factor of P_2/P_1. Tides may not have enough time to circularize the orbit at a relatively low eccentricity before REOs drive the orbit to higher eccentricities. Because REOs can reduce $(1 - e_1)$ by a factor of $\sim$5, this results in a reduction in $t_{\rm TF}$ by an order of magnitude. The orbit will thus circularize more rapidly and be brought into a closer orbit than it would by KL oscillations calculated in the secular approximation.

ACKNOWLEDGEMENTS

REFERENCES

Aarseth S. J., 2003, Gravitational N-Body Simulations. Cambridge Univ. Press, Cambridge
Aarseth S. J., 2012, MNRAS, 422, 841
Amaro-Seoane P., 2012, preprint (arXiv:1205.5240)
Amaro-Seoane P., Gair J. R., Freitag M., Miller M. C., Mandel I., Cutler C. J., Babak S., 2007, Class. Quantum Gravity, 24, 113
Amaro-Seoane P., Sesana A., Hoffman L., Benacquista M., Eichhorn C., Makino J., Spurzem R., 2010, MNRAS, 402, 2308
Amaro-Seoane P. et al., 2013a, GW Notes, 6, 4
Amaro-Seoane P., Sopuerta C. F., Freitag M. D., 2013b, 429, 3155
Antonini F., Perets H. B., 2012, ApJ, 757, 27
Antonini F., Faber J., Gualandris A., Merritt D., 2010, ApJ, 713, 90
Antonini F., Murray N., Mikkola S., 2014, ApJ, 781, 45
Blaes O., Lee M. H., Socrates A., 2002, ApJ, 578, 775
Blanchet L., 2006, Living Rev. Relativ., 9, 4
Bode J. N., Wegg C., 2014, MNRAS, 438, 573
Brem P., Amaro-Seoane P., Sopuerta C. F., 2014, MNRAS, 437, 1259
Brown D. A., Zimmerman P. J., 2010, Phys. Rev. D, 81, 024007
Fabrycky D., Tremaine S., 2007, ApJ, 669, 1298
Ford E. B., Kozinsky B., Rasio F. A., 2000, ApJ, 535, 385
Ford E. B., Kozinsky B., Rasio F. A., 2004, ApJ, 605, 966
Fregeau J. M., Cheung P., Portegies Zwart S. F., Rasio F. A., 2004, MNRAS, 352, 1
Gough B., 2009, GNU Scientific Library Reference Manual, 3rd edn. Network Theory Ltd
Gould A., 2011, ApJ, 729, L23
Gültekin K., Miller M. C., Hamilton D. P., 2004, ApJ, 616, 221
Hamers A. S., Pols O. R., Claeys J. S. W., Nelemans G., 2013, MNRAS, 430, 2262
Hoffman L., Loeb A., 2007, MNRAS, 377, 957

Holman M., Touma J., Tremaine S., 1997, Nature, 386, 254

Hut P., 1981, A&A, 99, 126

Hut P., 1982, A&A, 110, 37

Ivanov P. B., Polnarev A. G., Saha P., 2005, MNRAS, 358, 1361

Iyer B. R., Will C. M., 1995, Phys. Rev. D, 52, 6882

Janka H.-T., Eberl T., Ruffert M., Fryer C. L., 1999, ApJ, 527, L39

Katz B., Dong S., 2012, preprint (arXiv:1211.4584)

Katz B., Dong S., Malhotra R., 2011, Phys. Rev. Lett., 107, 181101

Kozai Y., 1962, AJ, 67, 591

Krymolowski Y., Mazeh T., 1999, MNRAS, 304, 720

Lidov M. L., 1962, Planet. Space Sci., 9, 719

Lithwick Y., Naoz S., 2011, ApJ, 742, 94

Merritt D., Alexander T., Mikkola S., Will C. M., 2011, Phys. Rev. D, 84, 044024

Mikkola S., Merritt D., 2008, AJ, 135, 2398

Mikkola S., Tanikawa K., 1999, MNRAS, 310, 745

Miller M. C., Hamilton D. P., 2002, ApJ, 576, 894

Mora T., Will C. M., 2004, Phys. Rev. D, 69, 104021

Naoz S., Farr W. M., Rasio F. A., 2012, ApJ, 754, L36

Naoz S., Farr W. M., Lithwick Y., Rasio F. A., Teyssandier J., 2013a, MNRAS, 431, 2155

Naoz S., Kocsis B., Loeb A., Yunes N., 2013b, ApJ, 773, 187

Paczynski B., 1986, ApJ, 308, L43

Perets H. B., Fabrycky D. C., 2009, ApJ, 697, 1048

Peters P. C., 1964, Phys. Rev., 136, 1224

Poincaré H., 1892, Les methodes nouvelles de la mecanique celeste. Gauthier-Villars et fils, Paris

Prodan S., Murray N., Thompson T. A., 2013, preprint (arXiv:1305.2191)

Raghavan D. et al., 2010, ApJS, 190, 1

Ruffert M., Janka H.-T., 1999, A&A, 344, 573

Ruffert M., Janka H.-T., Schäfer G., 1995, Ap&SS, 231, 423

Ruffert M., Janka H.-T., Schaefer G., 1996, A&A, 311, 532

Seto N., 2013, Phys. Rev. Lett., 111, 061106

Shappee B. J., Thompson T. A., 2013, ApJ, 766, 64

Soderhjelm S., 1975, A&A, 42, 229

Thompson T. A., 2011, ApJ, 741, 82

Wen L., 2003, ApJ, 598, 419

Will C. M., 2011, Proc. Natl. Acad. Sci., 108, 5938

Wu Y., Murray N., 2003, ApJ, 589, 605

Wu Y., Murray N. W., Ramsahai J. M., 2007, ApJ, 670, 820

APPENDIX A: DETAILS OF THE NUMERICAL METHODS

We have extended FEWBODY to include PN force terms up to order 3.5, presently the state of the art. Due to their length, we do not reproduce the terms here (the third-order term alone spans more than a page), but instead refer the reader to equations 182, 183, 185, and 186 of Blanchet (2006). These terms are conjectured to accurately reproduce GR effects to within several Schwarzschild radii. Though analytic error estimates do not exist in the literature, comparisons of PN calculations with direct integration of the Einstein field equations support the consensus that the PN terms are effective to within this range (Will 2011).

The PN terms are stronger functions of velocity and radius than the Newtonian term. Consequently, the inclusion of the PN terms makes integration of the orbits much more difficult, particularly for highly eccentric orbits where the radial distance and velocity are both changing very rapidly. Thus, while the PN terms might in principle be accurate down to several Schwarzschild radii, in practice the efficient computation of the orbit may limit the regime of applicability.

These difficulties are compounded by the roundoff error introduced by integrating close encounters far from the origin (see, e.g. Mikkola & Merritt 2008 for further discussion). If the positions of two nearby objects are represented with respect to a distant origin, the numerical precision is reduced by roughly the ratio of the distance of the two objects from the origin to their separation. (For example, if a computer has only four digits of precision and two objects are separated by 1.234×10^{-3} and are at a distance of 1 from the origin, their positions must be represented by 1.001, leading to a loss of three digits.) In practice, this can lead to a loss of six or seven orders of magnitude of precision and can render the evolution of high-eccentricity systems intractable. In general, roundoff error in N-body dynamical simulations can be avoided with some variation of algorithmic regularization (see, e.g. Mikkola & Tanikawa 1999; Aarseth 2003). However, because we are only concerned with the special case of hierarchical triple systems, we have modified FEWBODY to avoid roundoff error by automatically recentring the triple on every step so that the centre of mass of the inner binary is placed at the origin.

To test the correctness of our implementation and to characterize its regime of accuracy, we run several numerical tests. We first examine the degree of energy conservation in orbits at several eccentricities when no PN terms are included and when non-radiative PN terms are included. We then show that the orbital decay due to the 2.5 order PN term closely matches analytic calculations. Finally we compare the results from FEWBODY to an octupole-order secular model in several simple cases to demonstrate that systems in which the approximations of the secular model are valid produce similar behaviour as direct three-body integration.

A1 Energy conservation

The most straightforward way to determine the numerical accuracy of an N-body integrator is to determine how well energy is conserved. Once the change in energy becomes non-negligible compared to the total energy it is certain that the calculated dynamics are qualitatively incorrect. Typical energy conservation tolerances are set at least several orders of magnitude below this point. The largest tolerance often invoked is of the order of 10^{-5}.

In ordinary integration (i.e. without taking a Kustannheimo–Stiefel or similar transformation), energy conservation is worst during close encounters of extremely eccentric orbits. Due to the steep $1/r^2$ profile of the gravitational force and the rapid change in r near the periapsis of a highly eccentric orbit, such orbits are difficult to calculate accurately. This problem is exacerbated with the introduction of PN terms since the PN terms are even stronger functions of distance and include strong velocity terms which vary rapidly as well. For an orbit with a given semimajor axis, there is thus a maximum eccentricity to which we can accurately integrate.

To estimate FEWBODY's numerical accuracy and determine this maximum eccentricity, we integrate 3×10^6 orbits (approximately one Hubble time) of two $10^7 \, M_\odot$ SMBHs with a semimajor axis of 1 pc and eccentricities ranging from $1 - e = 1$ to 10^{-5}. This system is the inner binary of the systems we integrate in Section 4. Since the triple systems we later integrate consist of a tertiary with a mass of $10^7 \, M_\odot$ at a distance of 20 pc, we offset the binary in these energy tests to a distance of 10 pc so as to account for roundoff error that will be present when we integrate the triple systems. This initial offset has only a negligible effect on the calculation, however, because our code automatically recentres the triple system on the centre of mass of the inner binary on every step so as to eliminate this roundoff error.

We perform these calculations both with and without the PN terms. In calculations with the PN terms, we exclude the odd-order 2.5 and 3.5 terms since these serve to describe the effects of
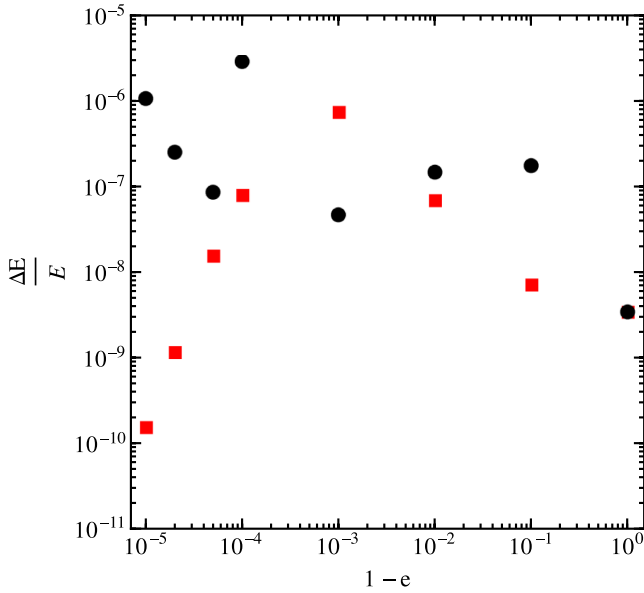
Figure A1. Energy conservation in FEWBODY for orbits over a range of eccentricities in the Newtonian case (red squares) and including non-radiative PN terms up to order 3 (black dots). We integrate the orbits for a Hubble time or for the gravitational radiation inspiral time, whichever is less. In all cases, energy conservation is better than 10^{-5}.

gravitational radiation. These force terms are not conservative and are therefore not appropriate in our checks for energy conservation. The accuracy of these odd terms is characterized in Appendix A2. We further note that when PN force terms are included in the integration, the expression for the energy changes. The energy term including PN terms up to third order is lengthy, so like the force terms, we do not reproduce it here, but instead refer the reader to equation 2.11 of Mora & Will (2004). (The energy term is also provided in equation 170 of Blanchet 2006, but is represented in a different gauge that contains an undesirable logarithm.)

For the low-eccentricity systems ($1 - e \geq 10^{-3}$), gravitational radiation is weak and so we integrate them for a Hubble time. The high-eccentricity systems will merge in under a Hubble time, however, so we simply integrate them for as long as it takes them to merge via gravitational radiation. The results of these integrations are presented in Fig. A1. The results from including the PN 1 term alone and from including just the PN 1 and PN 2 terms are very close to the results from including all three PN terms. They are therefore not displayed in Fig. A1. As expected, FEWBODY conserves energy best at low eccentricities. At high eccentricities, energy conservation is also quite good because only a small number of orbits need to be integrated. At all eccentricities, however, FEWBODY performs the integration for the necessary number of orbits and conserves energy to well under 10^{-5} (and often much better).

A2 Inspiral time

To test the accuracy of the radiation reaction terms we compare the orbital decay of a highly eccentric orbit to the analytic expressions of Peters (1964). From Peters (1964), the semimajor axis and eccentricity evolution of the orbit are described by the following two differential equations:

$$\left\langle \frac{da}{dt} \right\rangle = -\frac{64}{5} \frac{G^3 m_1 m_2 (m_1 + m_2)}{c^5 a^3 (1 - e^2)^{7/2}} \left(1 + \frac{73}{24} e^2 + \frac{37}{96} e^4 \right),$$

$$\left\langle \frac{de}{dt} \right\rangle = -\frac{304}{15} e \frac{G^3 m_1 m_2 (m_1 + m_2)}{c^5 a^4 (1 - e^2)^{5/2}} \left(1 + \frac{121}{304} e^2 \right).$$

The orbital decay time of the system is given by the integral

$$T(a_0, e_0) = \frac{12}{19} \frac{c_0^4}{\beta} \int_0^{e_0} \frac{e^{29/19} \left[1 + (121/304) e^2 \right]^{1181/2299}}{(1 - e^2)^{3/2}} \, de,$$

where

$$\beta = \frac{64}{5} \frac{G^3 m_1 m_2 (m_1 + m_2)}{c^5},$$

and

$$c_0 = \frac{a_0 (1 - e_0^2)}{e^{12/19}} \left(1 + \frac{121}{304} e^2 \right)^{-870/2299}.$$

To compare FEWBODY to the analytic results, we calculate the evolution of the orbital parameters of the orbit of two $10^7 \, \mathrm{M_\odot}$ SMBHs with a semimajor axis of 1 pc and an initial eccentricity of $1 - e = 10^{-4}$. For the purposes of this comparison, we perform the FEWBODY calculation with the 2.5 PN term alone. This is because Peters (1964) assumes that the orbits are Keplerian and calculates the gravitational wave power in the quadrupole approximation. For very eccentric orbits, the deviation from a perfect ellipse manifests itself as a longer dwelling time at periapsis. Since most of the gravitational radiation is emitted near periapsis, a fully relativistic orbit results in more radiation emitted than Peters (1964) predicts. As the 2.5 PN term is the only term that captures quadrupole radiation emission, this is the only term consistent with the assumptions of Peters (1964).

We find that the difference in the overall merger time between FEWBODY and Peters (1964) is less than 10^{-3}. We believe this discrepancy is due to the fact that FEWBODY treats the energy loss more realistically by emitting most of the orbital energy during passage through periapsis. Peters (1964), however, assumes that energy loss is continuous throughout the orbit. For very eccentric orbits like the ones we are modelling, FEWBODY's treatment leads to stepwise changes in the orbital parameters, whereas Peters (1964) assumes that these orbital parameters vary continuously across the entire orbit. Over many orbits, this difference manifests itself in small discrepancies in the orbital parameters between the two calculations.

During most of the orbit the semimajor axis calculated by FEWBODY is within 10^{-2} of the semimajor axis predicted by Peters (1964). At the end of the inspiral the discrepancy is much worse, but this is simply because the overall merger time of the orbit is slightly different between FEWBODY and Peters (1964). Although we therefore cannot adequately test FEWBODY in this regime, however, we are not interested in the precise dynamics prior to merger, only the overall merger time.

The orbital decay including only the 2.5 PN term is presented in Fig. A2. The effect of adding the additional PN terms is a 0.5 per cent change in the overall merger time. At higher eccentricities the other PN terms become stronger and yield even larger discrepancies.

A3 Comparison to the secular approximation

If any changes to the orbital parameters in a hierarchical triple are slow compared to the outer orbital period, the orbits need not be integrated directly, but instead can be calculated from a time-averaged Hamiltonian (e.g. Blaes et al. 2002). Although we show in this paper that this approximation breaks down in important regions of parameter space, there are broad regimes in which this approximation works well. In particular, the secular approximation
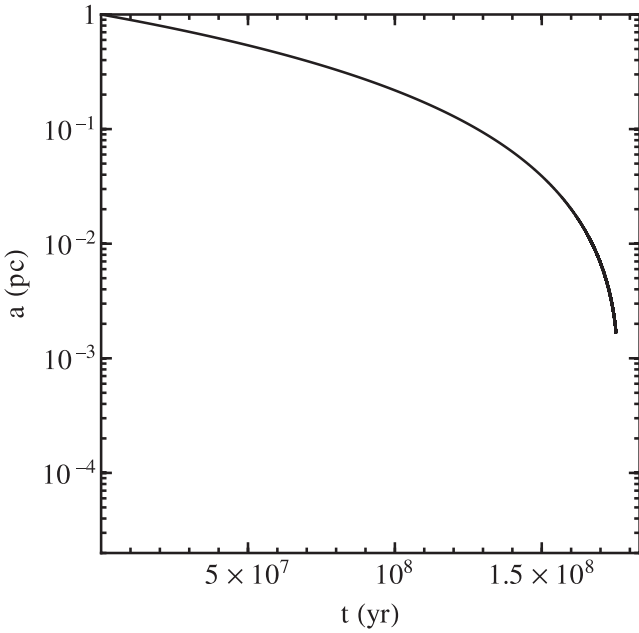
Figure A2. The evolution of the semimajor axis of a binary of two $10^7 \, M_\odot$ SMBHs with an initial semimajor axis of 1 pc and an initial eccentricity of $1 - e \sim 10^{-3}$. For purposes of comparison with Peters (1964), the calculation shown includes only the 2.5 PN term. The difference between our results and Peters (1964) is much less than the thickness of the line. We also calculate the evolution using all PN terms up to and including PN 3.5. In this experiment, the difference in the merger time between this calculation and the full PN calculation is 0.5 per cent. For clarity, we omit displaying the evolution in the full PN approximation. At higher initial eccentricities the discrepancy between the full PN calculation and the 2.5 PN term alone is larger. The inner binaries that we examine in this paper begin to suffer copious energy loss due to gravitational radiation at an eccentricity of $1 - e \sim 10^{-4}$. At this eccentricity, the difference between the full PN calculation and the 2.5 PN approximation in Peters (1964) is ~ 5 per cent.

Table A1. Initial conditions for a system that undergoes weak KL oscillations. See Fig. A3 for the evolution of this system.

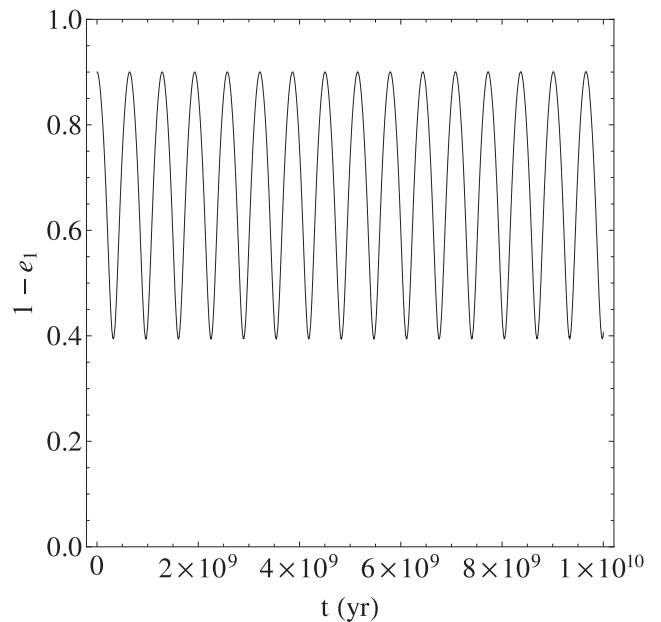| Parameter	Value
m_1	$10^7 \, M_\odot$
m_2	$10^7 \, M_\odot$
m_3	$3 \times 10^6 \, M_\odot$
a_1	1 pc
a_2	20 pc
e_1	0.1
e_2	0.2
g_1	0
g_2	0
$\cos i$	0.5

Figure A3. The evolution in eccentricity of a system undergoing KL oscillations. This system does not exhibit oscillations to extremely high eccentricities, so it is in the regime in which the secular approximation is valid. Properties of this system are listed in Table A1. We evolved this system for 10^{10} yr using both the secular model of Blaes et al. (2002) and by performing the direct three-body integration using FEWBODY. The difference between the two techniques is much less than the thickness of the line and amounts to an ~ 0.1 per cent offset in time at the end of the calculation. The difference between the calculation in the secular approximation and the direct three-body integration is explored further in Fig. A4.

works very well when the KL mechanism does not excite extremely high eccentricities.

We here show the agreement between the orbital evolution in the secular approximation with the direct three-body integration. For the secular approximation, we use the formalism of Blaes et al. (2002), which is an octupole-order calculation that includes GR precession and gravitational radiation. (Note that Blaes et al. 2002 use the equations of GR orbital decay from Peters 1964. As discussed in Appendix A2, this slightly underpredicts the merger time for highly eccentric orbits.) The orbital evolution is compared to the explicit orbit integration using FEWBODY for a slowly varying hierarchical triple undergoing KL oscillations. Because the Hamiltonian in Blaes et al. (2002) uses the results from Peters (1964) to account for gravitational radiation, the only radiation term we include is PN 2.5. Similarly, the formalism for handling apsidal precession in Blaes et al. (2002) is equivalent to the first PN term. Thus, the only PN terms we include in this comparison are PN 1 and PN 2.5.

We calculate the evolution of a triple system in which the KL mechanism is present, but does not excite extremely high eccentricities. Properties of this system are listed in Table A1. We evolve the system for 10^{10} yr, or about 15.5 KL cycles. The eccentricity evolution of both calculations is presented in Fig. A3. The difference between the two systems is equivalent to a 0.1 per cent scaling in time. This small difference is due to the fact that FEWBODY be-

gins the integration with each object at a random point along its orbit and at random longitudes of ascending node. These different starting conditions yield slightly different orbits. The initial phases of the orbits and longitudes of ascending node do not impact the orbit-averaged evolution of Blaes et al. (2002). The variation due to these random initial conditions from one realization to the next is consistent with the difference between any particular realization and the orbit-averaged calculation.

To more clearly illustrate the differences between the secular and FEWBODY calculations, we run the FEWBODY calculation 100 times with random initial mean anomalies for each run. The variation in the evolution of the eccentricity of the inner orbit is shown in
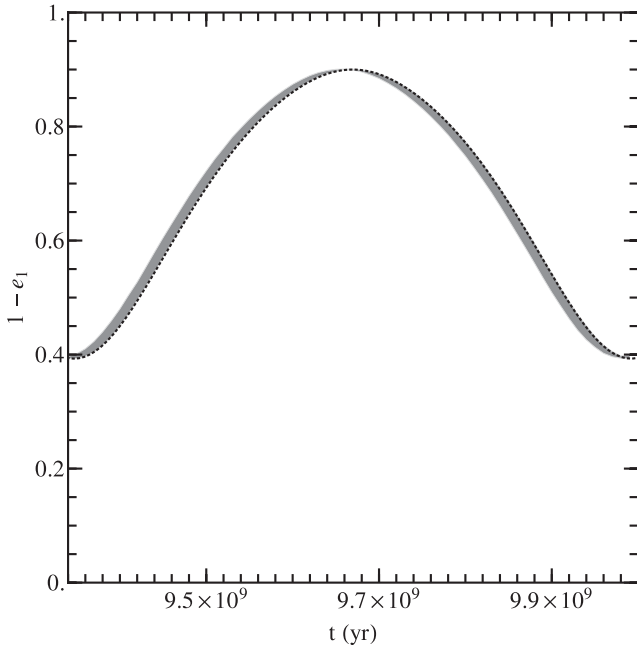
Fig. A4. The magnitude of this variation is an ∼0.15 per cent scaling in the time, which amounts to an offset of ∼15 Myr after 10^{10} yr. The evolution predicted by the secular calculation is consistent with the range calculated by FEWBODY.

Figure A4. The final moments of the evolution in eccentricity of the system presented in Fig. A3. Properties of this system are listed in Table A1. The secular calculation (dotted line) is shown with the results of 100 runs using FEWBODY (grey region). The orbits of the triple system in each run were given random initial mean anomalies. The variation in the orbital evolution due to these random initial mean anomalies results in an ∼0.15 per cent offset in time. The difference between the secular calculation and any given calculation using FEWBODY is consistent with this variation.

This paper has been typeset from a TEX/LATEX file prepared by the author.